



ELSEVIER

Physica D 106 (1997) 375–388

PHYSICA D

Computational modeling of mound development in *Dictyostelium*

Herbert Levine^{a,*}, Lev Tsimring^a, David Kessler^b

^a *Institute for Nonlinear Science, University of California, San Diego La Jolla, CA 92093-0402, USA*

^b *Department of Physics, Bar-Ilan University, Ramat Gan 52900, Israel*

Received 31 January 1996; revised 20 September 1996; accepted 21 October 1996

Communicated by H. Flaschka

Abstract

One of the structures seen during the course of *Dictyostelium discoideum* development is the loose aggregate or early mound structure. In this work, we attempt to simulate the formation of this three-dimensional mound by a model which incorporates cAMP chemical signaling and resultant cell motions due to chemotaxis. Simulation results are compared to measurements of the mound morphology as determined by confocal fluorescence microscopy. Good agreement is obtained only if the cells exhibit an adaptive response to high cell density and change their basic motion patterns. We argue that in the actual biological system, this occurs because the high resting value of cAMP in the mound can effectively saturate the high-affinity receptors responsible for aggregation stage dynamics. Tests of our ideas using mutant cell lines are briefly discussed.

1. Introduction

The morphology changes that result from the starvation-induced development of *Dictyostelium discoideum* are truly remarkable (see [1]).¹ Under the influence of an unfolding genetic “program”, this system progresses in a period of 24 h from a set of weakly interacting solitary amoebae to a fully differentiated fruiting body. Along this developmental path, the morphology changes from a uniform two-dimensional density to a set of incoming streams to a three-dimensional mound; this mound then exhibits tip elongation, slug forma-

tion, and eventually reaches the aforementioned final state.

Much is understood about the early stages of this pattern formation process. In particular, cells are signaled to move towards nascent aggregates by waves of cAMP [2].² Once cell motion becomes dominated by chemotaxis towards the cAMP wave source, the cell density field undergoes a transverse clumping instability which drives stream formation [3–5]. Of course, there is work still needed on formulating quantitatively reliable models, especially the manner in which positive feedback from the signal receptors affects further genetic expression. However, it is fair to say that we have in hand a qualitatively

* Corresponding author.

¹ For a general introduction see Loomis (1992) and Bonner (1967) in [1]; for other reviews see Devreotes (1989), Newell (1981) and Darman and Brachet (1978) in [1].

² Other researchers have inferred the existence of cAMP wave by its effect on the cell image in a dark-field microscope setup, see e.g. Alacrantra and Monk in [2].

valid picture of this early stage of Dictyostelium morphogenesis.

As the aggregate increases in size and expands into the third dimension, additional mechanisms come into play to determine the organism morphology. Specifically, cells now are in direct proximity with others and form adhesive contacts. These contacts bias the motion of cells in the multicellular state and differential adhesion between different cell types may offer clues for cell sorting.³ At least until such time as elastic forces associated with sheath formation might begin to play an important role in shaping the mound (the “tight” aggregate stage, at 10–12 h post starvation), the overall morphology must arise due to a competition between chemotaxis and adhesion. This competition is the subject of this paper.

It is worth outlining the methodology which we have brought to bear on this issue. In Section 2, we describe experiments on mound morphology conducted via a Dictyostelium cell-line⁴ which expresses green fluorescent protein (GFP [7]) under the actin-15 promoter. These experiments have concentrated on determining the shared characteristics of many mounds at the 8–10 h (post starvation) “loose” aggregate stage. We will see that the morphology is flat-topped, with sides that slope downward, typically in a manner consistent with a zero degree contact angle with the substrate. It is these features that we attempt to reproduce via a computational model discussed in the following sections. Extensions of our measurements so as to enable single cell-tracking⁵ and subsequent comparisons to simulated trajectories are in progress and will not be discussed further in this publication.

Our computations have been performed with the recently introduced [9,10] “bion” paradigm for Dictyostelium. In this approach, cells are represented by individual automata which respond to signals in (an internal-state dependent manner) by moving,

emitting chemical signals and changing their internal state. Treating the cells as separate discrete entities [11,12]⁶ has significant advantages over the usual continuum description [13] of a cell density field coupled to reaction–diffusion equations for the signal system. In particular, it is straightforward to account for the transport of state information (such as receptor desensitization) via the motion of cells, and also for the bias of cell motion via local adhesive interactions. Also, mixing of wild-type cells with mutants with altered response rules can easily be encompassed, without multiplication of the number of independent fields as would occur in the aforementioned continuum description. Finally, this type of model is essential when one extends the computations to include differentiation of cells into the pre-spore or pre-stalk cell types in response to external chemical signals (see e.g. [14]). The details of our bion algorithm are given in Section 3.

The major result of this work concerns the need for reduced signaling and/or chemotaxis in the mound interior if the model is to accurately reflect the measured morphology. We propose that cells reduce their tendency to move toward the actual center of the mound as they enter the high cell density region. This might be due to simple adaptation of the cAMP response (essentially never allowing the receptors to re-sensitize) at high cAMP concentration, or due to a (hypothesized) repulsive chemical signal or perhaps a direct response induced by high cell density – the model is unable at its current level of sophistication to be more discriminatory. Incorporation of such an effect then yields simulated mounds in good agreement with measured ones. Caveats (explained below) involving our simplified treatment of signaling notwithstanding, we believe that our results lead to some very specific predictions that eventually could be tested by using developmental mutants. Possible tests of our ideas are discussed in the concluding section of this paper.

³ It is well-established that differential adhesion can drive cell sorting in other biological contexts (see e.g. [6]) Whether this is an important mechanism in Dictyostelium is an open issue.

⁴ We would like to thank R. Kay for providing us with this strain.

⁵ This has already been demonstrated in McNally lab by Doolittle et al. [8].

⁶ Previous attempts at developing many-cell models include the papers in [11]. These papers did introduce the idea of a single cell as a dynamical entity but did not proceed to perform semi-realistic two-dimensional simulations.

2. Experiments on mound morphology

We grew *Dictyostelium* cells in HL-5 medium [15] (shaking culture) to a density of 3×10^6 – 5×10^6 cells/ml. The cells themselves were Ax2 strain cells into which was inserted the gene for green fluorescent protein, driven by the actin-15 promoter. After growth, cells were starved by removing the HL5 and re-suspending in phosphate buffer. We then spread 1×10^7 – 2×10^7 cells along with about 2 ml of buffer onto a filter pad with an absorbent pad backing. The filter was placed in a humid chamber and the cells were developed for 8 h.

Imaging of mounds was accomplished by removing the pad from the chamber and placing it onto the stage of a confocal microscope. Fluorescence was excited by using a 488 nm laser line. With the 20 \times air objective, single early mounds typically took up a significant portion of the field of view of 640×480 pixels, where each pixel is $0.66 \mu\text{m}$. With a slit size of $15 \mu\text{m}$, sufficient resolution was obtained with optical slices separated by $3 \mu\text{m}$. Characteristic resolution of confocal imaging was estimated by observing small fluorescent beads and it was of the order of $3 \mu\text{m}$. The total number of slices was determined by scanning through the mound until no appreciable light could be seen either above or below the mound for the top and bottom slices respectively; a typical number obtained in this manner was 30 slices.

In this work, we were primarily concerned with three-dimensional mound morphology at this loose aggregate stage. We selected mounds that had “absorbed” most of their incoming streams and formed images as described above. To get the three-dimensional shape, we plotted light intensity vs. slice number at fixed x, y positions; a graph of one such x, y is given in Fig. 1. We then picked a threshold at a fixed fraction of the maximal intensity as a function of z to define the upper and lower surfaces; the threshold was optimized to get a flat bottom. This simple procedure accounts for the fact that even with the confocal setup the resolution in z is significantly worse than that in a fixed plane – this can be seen by measuring the point-spread-function of small beads. Based on our bottom reconstruction, we estimate that

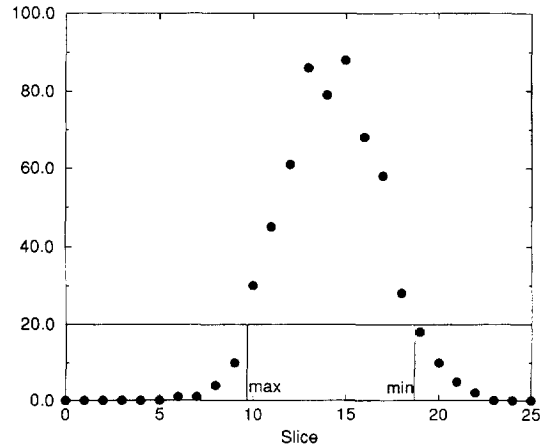


Fig. 1. Distribution of brightness of light over a stack of slices at a fixed (x, y) point. A solid lines indicates an ad hoc threshold used to determine the positions of top and bottom of the mound.

the height vs. x, y is being determined to an accuracy of $\pm 3 \mu\text{m}$ by our approach. This is quite sufficient to resolve the global morphological features of interest here.

Figs. 2 and 3 show a set of three mounds, first in $x-z$ view and then in a perspective view of the surface reconstruction. The mounds are all flat-topped, with edges that smoothly slope down to meet the oncoming streams. The latter fact is characteristic of practically all loose aggregates we have measured – the formation of a sharper edge with an apparently finite contact angle leading to a flattened hemispherical morphology happens later in the development cycle. Fig. 4 shows a morphology time sequence which demonstrates this “sharpening”, as a single loose aggregate breaks up into several sharper tight mounds.

Under our developmental conditions, some but not all of the loose aggregates show distinct evidence of spiraling cell motion [8,16,17]. Often, one can detect a spiraling mound by the existence of one or many streams which “wrap” mound the mound. For simplicity (and to compare to the simulations described subsequently), we have restricted our measurements to mounds with no “obvious” spiraling. This does not mean that individual cells are not moving in spiral trajectories, merely that one could not see any highly coherent motion of cells over the entire mound.

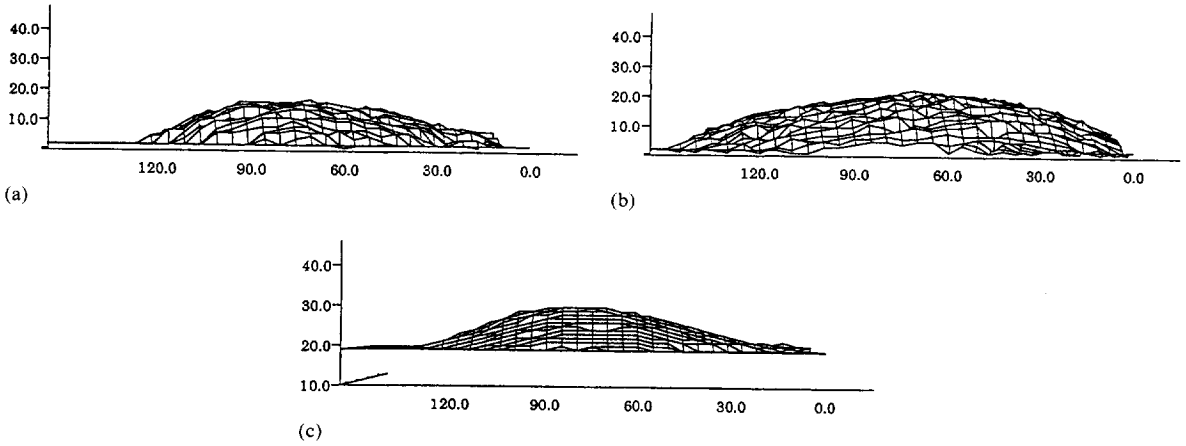


Fig. 2. Side views of three different mounds at the “loose aggregate” stage of mound formation. Flat tops and small contact angles are characteristic features of all observed mounds.

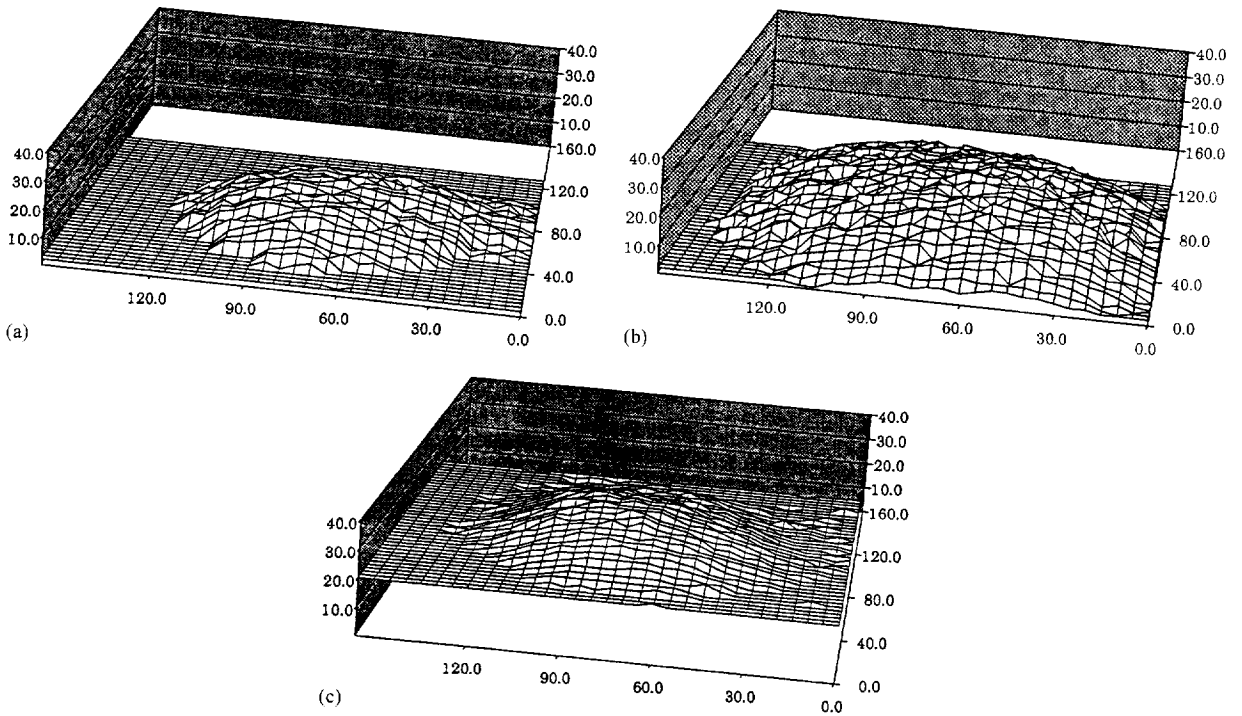


Fig. 3. Perspective views of the same three mounds as in Fig. 2.

To recap, we have measured early mound shapes for a specific developmental protocol and obtained accurate three-dimensional information. Reproducible features of these mounds include their flatness, their

sloping edges (skirts) and their circularity. Any model of cell signaling and chemotaxis should be able to explain/reproduce these features. We now turn to a discussion of how we model *Dictyostelium* aggregation.

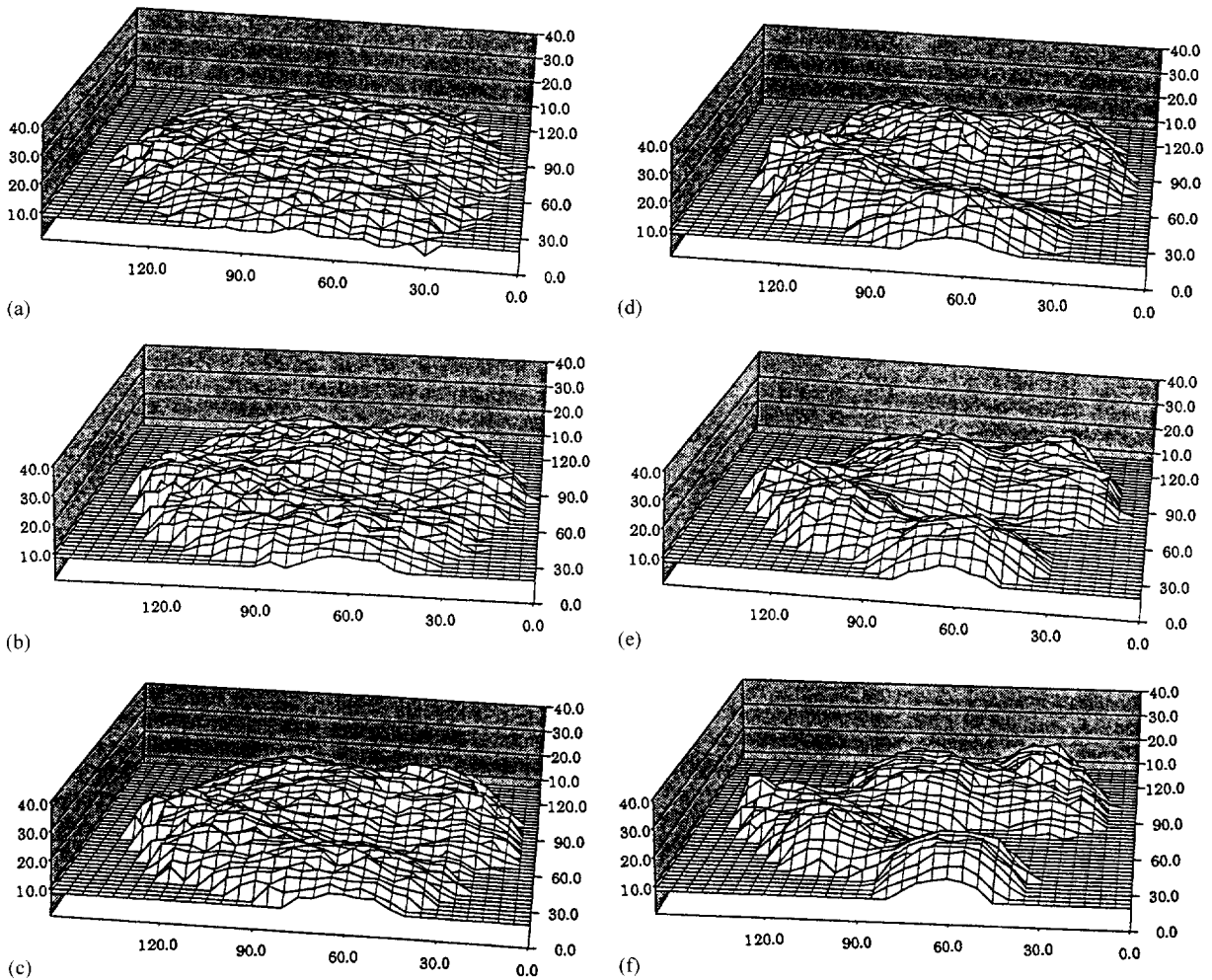


Fig. 4. Time evolution of a mound surface: six snapshots approximately 10 min apart. In this example a mound eventually splits into several smaller pieces; this may be indicative of aggregation with the spiral cAMP wave with a central low-density region.

3. Computational model

In several recent publications [9,10], the idea was advanced of using a hybrid scheme (treating the cells as independent automata and chemical diffusion via a discretized partial differential equation method) to simulate *Dictyostelium* development. In that work, the formation of streams from an initially uniform cell density field was shown to follow automatically from the joint effects of excitable waves and chemotaxis. This result was in agreement with calculations [3] of a linear stage of the streaming instability in a coupled

cell-density, chemical signaling model and has been subsequently reproduced in simulations based on the continuum reaction–diffusion framework [4,5].

In addition, more subtle aspects of stream patterns were accurately simulated – these include the presence of a small central hole in the density field produced by a spiral wave signaling pattern [18], the lack of dependence of streaming on cell–cell adhesion [19], the lack of sorting of signal-deficient but chemotactically normal cells from wild-type and the dependence of stream density on cell density. The same model with an additional feedback mechanism controlling gene

expression (for the signaling system) is also able to simulate the transition from random “firing” to large spiral and target patterns at the initial stage of development [20]. Work is continuing on trying to be able to predict the typical spacing between aggregation centers and the morphology (e.g. spirals vs. targets) of the excitable waves.⁷

In simulating mound formation, we will need to extend the previous work to encompass the effects of cell–cell adhesion and the ability of cells to climb on top of other cells, i.e. to make a three-dimensional structure. To get started, let us first review the ingredients of the model whose results were described above. The first component of our *Dictyostelium* model consists of the signaling dynamics. It is well established that the cyclic AMP–cell receptor system falls into the general class of excitable chemical dynamics. These are systems which will propagate nonlinear waves in response to an above threshold perturbation. In this case, the wave is sustained by each cell binding an above threshold cAMP concentration, turning on a cAMP production and excretion facility, and then relaxing back to the unexcited state over a finite refractory period. Typical numbers for this signaling system are wave speeds of 300 $\mu\text{m}/\text{min}$, with cAMP concentration oscillating from 10^{-8} to 10^{-6} M.

To mimic this behavior, we place independent computational “cells” (which we refer to as bions) randomly on a two-dimensional hexagonal lattice with density ρ ; typically ρ should be 5–20%, if we interpret our density as equal to the relative amount of intracellular to total area in an aggregating colony. In addition, cyclic AMP concentration c is taken to obey a (discretized) diffusion equation

$$\frac{\partial c}{\partial t} = a^2 \nabla^2 c - \Gamma c + \text{sources}, \quad (1)$$

where we have normalized the diffusion constant to a^2 (the square of the lattice size); the decay is due to the degradation of cAMP by phosphodiesterase, here assumed to be at a fixed uniform concentration.

⁷ There appears to be a transition between target-dominated and spiral-dominated wave fields as the cell density is increased [21].

The second component of our model endows each bion with a new sensor and a chemotactic motion rule. To wit, the gradients of cAMP are computed and compared to a motion threshold c'_T/a . It is reasonable to expect that this threshold is of order $c_0/(\text{cell size}) \sim c_0/(\text{lattice spacing})$ since the sensing of the gradient most likely arises due to differential binding of the cAMP receptors on opposite sides of the cell [22]. In our model, cell motion is implemented as follows. The magnitude of the gradient is measured by standard finite differencing and the threshold condition is evaluated. If the cell “decides” that it should move, we determine the direction of the gradient and pick two possible move directions by the largest and second largest projections of the gradient onto the six hexagonal lattice vectors. Once set, these directions are not altered for a given active cycle. The computational cell will then attempt to move in one of these two directions for as long as it remains active. Once it succeeds in moving (as determined by space availability as detailed below), it cannot move again until it re-enters the active phase one (or more) cycle(s) later. For motion limited to two dimensions, the motion is carried out if and only if the “target” site is vacant.

The model as stated contains a variety of different parameters related both to the signaling system and the chemotactic motion. Most of these can be taken directly from experiments; for example, the values of the refractory period (t_R), the amount of cAMP released per excitation (Δc) as compared to the threshold (c_T) are all known. Other features are not as well characterized, such as the exact manner in which cell–cell interaction affects chemotaxis; for these we have made what we feel to be reasonable guesses based on available video recordings of aggregating cells. It is crucial to understand, though, that goal here is not to make a totally faithful and quantitatively reliable model which mimics the complex biochemistry underlying the aggregation stage dynamics. Instead, our goal is to investigate which mechanisms must be included in a model for getting qualitative agreement with what actually occurs in *Dictyostelium*. In other words, we ask about the ability of the model with *any* reasonable parameter choice to reproduce certain experimentally observed facts; this issue is studied as

a way of trying to connect mechanism with consequence in a manner which does not rely on all the precise details of the model, since those details cannot in any case be quantitatively accurate. As an example of this type of logic, one can consider the fact that cAMP waves annihilate each other upon contact. It is by now well understood that this phenomenon requires for its explanation the existence of a refractory period for wave excitation, independent of any of the details of an underlying excitable media model. It is this level of understanding that we hope to achieve for the pattern formation problem in *Dictyostelium*.

As already mentioned, several previous publications [9,10] discussed the behavior of this model as compared to two-dimensional aggregation patterns. This discussion will not be repeated here. Instead, we turn now to extensions of this approach to encompass motion of cells into the third dimension and the building of the mound.

4. Three dimensionality

In the current work, we are specifically interested in building three-dimensional structures. The largest simplification that we make is that we continue to treat the chemical field as two-dimensional that is, we assume that diffusion is fast enough to smooth out gradients in the vertical direction since the (early) mounds we study are very flat. This will undoubtedly cease to be true as we progress to the tight mound stage and vertical gradients presumably begin to play a critical role in cell-specific sorting. For most of our simulations, we assume that all of the emitted chemical from cells in a specific horizontal position are added together to give the change in two-dimensional concentration; this roughly corresponds to the notion that there exists a thick layer of fluid covering the aggregate and so there is no additional “space” for chemical introduced as the mound grows vertically. We have checked (see later) that switching to the opposite assumption, namely that the fluid layer is very thin and therefore the chemical concentration will be reduced via vertical spreading as the mound grows, does not alter our conclusions. Of course it will be important to extend

our model to incorporate full three-dimensional cAMP diffusion. Note though that the most natural direction for the vertical component of the gradient is upward, since chemical can leak through the bottom into the substrate but not upward into the air; this will only enhance the tendency of mounds to grow and be too sharp in the absence of adaptation, a result we shall soon encounter. This fact, plus the lack of any experimental indication whatsoever that cells at this stage move vertically due to chemical gradients give us confidence that our conclusions are not being affected by this simplification.

Now, we extend our motion rule to allow “climbing” which we define to be a change in the z position of a cell by ± 1 . Again, there is a lack of detailed data upon which to base our rules, so we proceed by making what we feel to be sensible hypotheses. If a cell attempts to move in a given direction (due to the aforementioned chemotactic response) and it cannot move to the desired position on the same z level, it will attempt to move up or down. Assuming that the proposed site is vacant, we compute the number of nearest neighbor cells in its current position and compare this to the number of nearest neighbor cells in the proposed new site. If the new site has more occupied neighbors, the move is accepted; if not, the move is accepted with probability $1 - \exp(-g/g_0(\Delta nn))$ where g is the magnitude of the gradient and $g_0(\Delta nn)$ is a threshold which depends on the change in nearest neighbor occupancy (Δnn). This mechanism accounts for the fact that climbing tends to decrease the number of nearest neighbors (in the simplest case, one cell climbing atop a nearby cell with no other nearby cells clearly has ($\Delta nn = 1$)) and hence is suppressed by cell–cell adhesion – this assumes the cells stick to the substrate about as well as they stick to each other which is reasonable for cells at the mound stage.

Finally, we add in a new dynamical feature, that of relaxation under purely adhesive forces in the absence of chemotaxis. Once cells enter the refractory stage, they do not attempt to move chemotactically. Instead we allow the cells at the top of columns to move to nearby columns if such a move would increase the overall number of adhesive contacts – we typically do this for 50 or so time steps Δt by picking a few

directions randomly and evaluating Δnn . This type of move is familiar from simulations of crystal surfaces relaxing via surface diffusion (see [23] and references therein). In the absence of any driving, this would give rise to an effective relaxation whereby perturbations in the profile would decay, with a rate depending on the fourth power of their wave vector. In Appendix A we present a simple analytical caricature of our hybrid model which describes the shape of a radially symmetric mound under a constant inward flux of cells and surface relaxation in a continuous limit. It can be readily seen that a sharp cusp is immediately formed in the center of the mound. This agrees with the results of simulations of the hybrid model.

In Section 5, we will discuss simulation results with this model and with a model with one additional extension. In the basic model, cells always proceed from refractory to quiescent after a fixed time interval. In the actual *Dictyostelium* amoebae, this progression is believed [24,25]⁸ to involve the re-sensitization of the signal transduction apparatus leading from receptor to cAMP production and to chemotaxis, after de-sensitization by the initial cAMP wave. This progression will not occur at sufficiently high resting cAMP concentrations. Hence the fact that the overall concentration rises inside the mound could interfere with the directed motion component due to chemotactic response. To include this effect, we have modified our simulation to prevent the clock which begins counting to the fixed end of the refractory period from starting this countdown until the concentration has gone below an upper threshold c_u which we take to be much bigger than the threshold c_0 . If a typical value of c_0 is taken to be 10 nM, c_u might be 10 μ M.

It is important to realize that any computer model of this type requires a variety of ad hoc choices regarding exactly how to implement motion, signaling, etc. We must therefore check that any results which emerge from simulational studies are not dependent on these small details and instead characterize behavior expected of the real biological system. Although we will not discuss them in any detail, we have performed a large number of simulations with small variations

of the above scheme (modifying the climbing rules or the relaxation steps, allowing limited time double occupancy, using a square lattice, etc.) to verify that our conclusions are not unduly influenced by non physical computational artifacts. We now turn to a discussion of our results for simulating mound morphology.

5. Simulation results

In Table 1, we list all the values of all parameters that characterize our model, as discussed in the previous section. Unlike real *Dictyostelium* cells, our model does not incorporate elaborate feedback loops which automatically adjust certain parameters (for example, the decay rate due to phosphodiesterase in response to cell density changes [26]) to enable aggregation and mound formation to occur over a wide range of conditions. Instead, we need to do this by hand. For example, if we change the cell density by a factor of 2, we must re-tune the decay rate in order to maintain integrity of the aggregation stage dynamics. The ability of real cells to compensate for change in environment is an important issue which is beyond the scope of this work – it does make the issue of getting semi-quantitative results from computational modeling more difficult than is often appreciated.

In Fig. 5, we show a sequence of surface reconstructions for a model which does not adaptively turn off chemotaxis and signaling as the cells enter the high density mound. The cells form streams rather

Table 1
Parameter values for mound formation program

Parameter	Description	Value
Δt	Time-step	0.12
t_s	Initial signal period	30
Γ	cAMP decay rate	0.5
ρ	Density	0.25
Δc	Total concentration release	300
t_A	Active time	2
t_R	Refractory time	18
L_x	Lattice size	100
N_{relax}	Number of relaxation time-steps	100
$\text{Relax}_{\text{try}}$	Attempts per relaxation step	8
g_0	Gradient threshold	2
$g[k]$	Weighting with adverse $\Delta nn = k$	$3k \times 10^5$

⁸ For a detailed model of signaling biochemistry see [24].

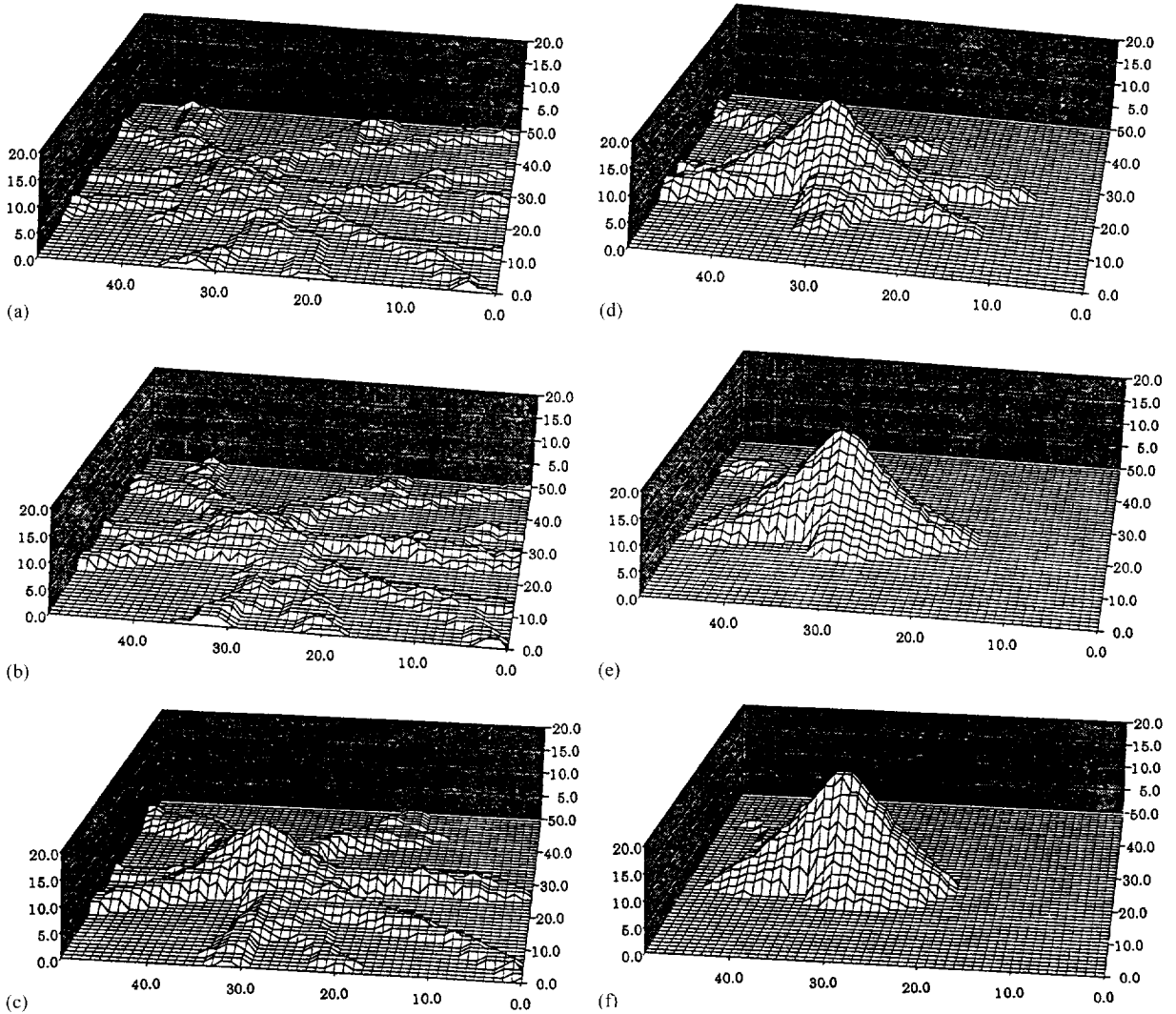


Fig. 5. Model simulation of mound aggregation: a sequence of snapshots, $t = 10$ (a), 20 (b), 40 (c), 60 (d), 60 (e), 100 (f). Parameters of the simulations are given in Table 1. Emission of cAMP does not saturate near the center of the mound, so a sharp tip is formed at the later stages (d–f).

quickly but climbing is suppressed to a significant degree until there is a large enough “puddle” of cells at the aggregation center. We should point out that the cells are responding to an assumed pacemaker cell (or clump of cells) which fires periodically and generates a target wave. Depending on cell density and specific *Dictyostelium* strain, the typical wave pattern seen experimentally is either target-like or spiral-like [21]; we have chosen to simulate target-wave mound formation. It would also be valuable to study whether we

expect any differences between target-wave or spiral-wave mounds, but we leave this for the future.

As the cells experience a large enough gradient to overcome the adhesion barrier to climbing, the overall mound rises into the third dimension. In this simulation, cells continue to move inward even as they enter the high density region. As one can see, the peak remains sharp, i.e. there is a maximum of curvature at the mound center. This result is independent of almost all the details in our simulation. For example, in Fig. 6

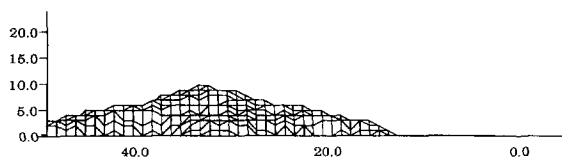


Fig. 6. Final stage of mound simulation with modified concentration equation, corresponding to three-dimensional cAMP spreading.

we show the final structure formed during a simulation where the cAMP is allowed to spread out in the vertical direction, corresponding to the assumption that the mound is much higher than any fluid layer covering the aggregate and hence more space is created for the chemical as the mound grows. Although there is some quantitative change, the sharpness of the peak is not diminished. In Appendix A, we present a simple mean-field analysis which explains why this result occurs generically in our class of models, as long as we do not reduce chemotactic motion near the mound center.

Given this set of results, it is clear that flat-topped mounds require an additional biological “control” mechanism. Specifically, we need to modify the cycle of cAMP production and cell motion so that the radially directed chemotactic component of the cell velocity diminishes on average as we approach the mound. In our *Dictyostelium* simulation, this can be accomplished in several ways. Perhaps most trivially, one could postulate the existence of a second chemical signal which accumulates in high density regions and turns off chemotaxis. There is some circumstantial evidence (based on simulations) for the existence of a repellent in patterns formed by bacterial chemotaxis [27], but no obvious biological correlate here. Instead, we use the same signal, cAMP, but introduce a saturation concentration such that we do not allow the cells to recover their response (after waiting the typical refractory period) until the concentration falls below this level. This mechanism affects the mound development in two ways. First, it reduces an average amount of cAMP emitted by cells in the high density region, thereby lowering the level of cAMP inside the mound and making its gradients shallower. Secondly,

the directed motion of cells itself is also suppressed. The exact procedure by which this was accomplished computationally was given in Section 4.

The results of the new simulation with the upper-threshold $c_u = 1700c_0$ are shown in Fig. 7. The difference is quite clear as now the top quickly flattens as the cells near the center lose directed motion. The final mound shapes are in qualitative agreement with the measured mounds described in Section 2. One can get similar results with the suppressor chemical described above or with other approaches that effectively amount to making the net flux approach zero in the mound center.

The actual structure we get is fairly sensitive to the value of c_u . If c_u is too high, the cAMP concentration never reaches the threshold, and we recover the previous findings. If c_u is too low, cells begin to lose signaling and chemotactic response in streams and significant numbers of cells are not incorporated into the central region (see Fig. 8). In fact, a mutant with this phenotype has recently been seen [28]. Our model is less sensitive to the details of the surface relaxation (for example, the number of tries that a cell makes to locally relax to a maximally contacted neighboring site only makes small quantitative changes in the results) and to the initial cell density or signaling parameters. Our basic result is therefore that the observed mound morphology specifically requires carefully balanced adaptation to high cAMP.

6. Discussion

In this work, we have attempted to model mound formation in *Dictyostelium* and compared our simulation results directly to experimental findings. Our computational methodology relies on using an automata model for cells as they interact with each other and cooperatively form the three-dimensional aggregate. The main advantages of this framework are the flexibility especially with regard to cell response and the direct relationship between assumptions regarding real-world cell behavior and computational parameters. These are in distinction to what occurs in usual continuum approaches to multicellular systems.

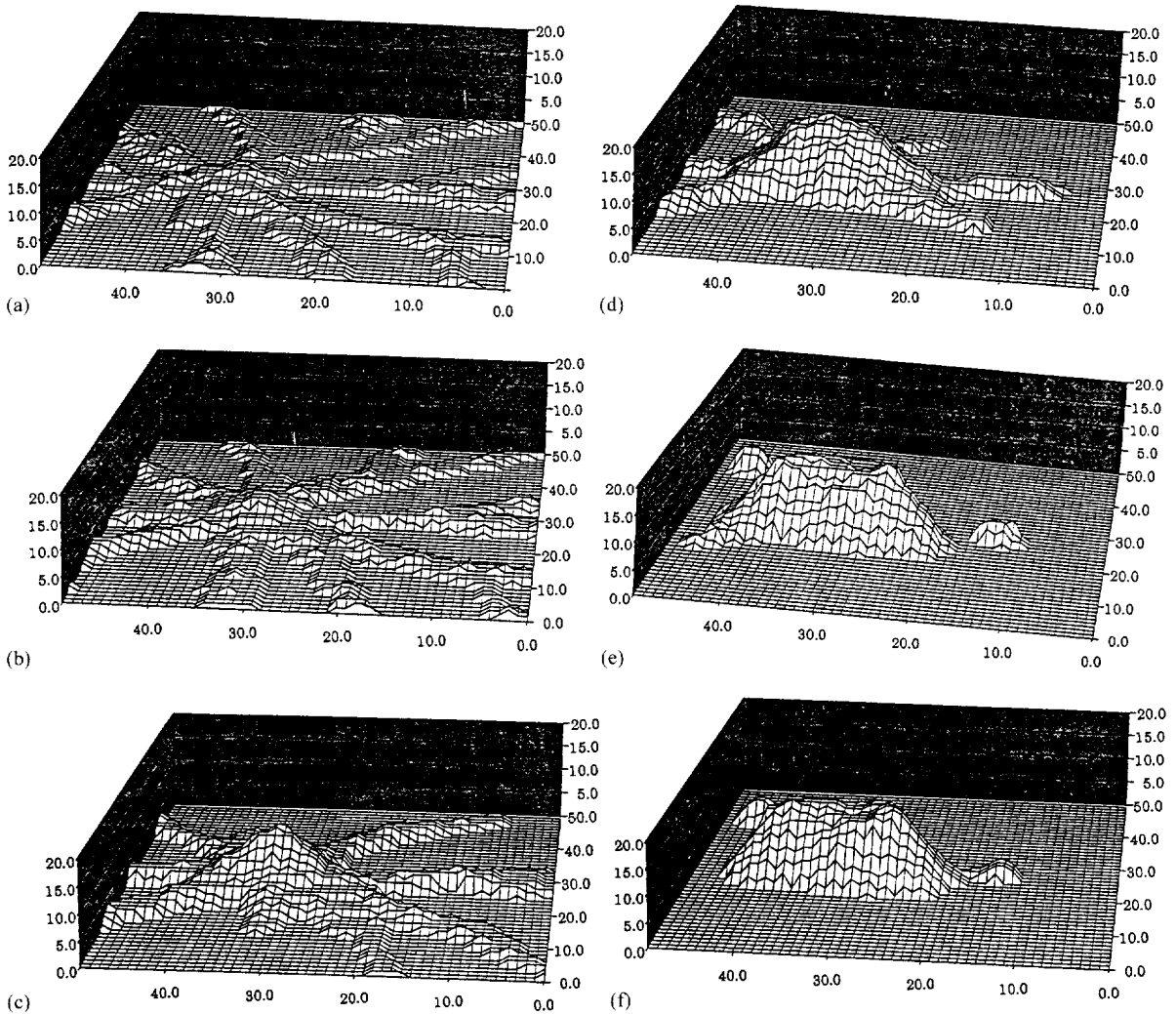


Fig. 7. Model simulation of mound aggregation: a sequence of snapshots, $t = 10$ (a), 20 (b), 40 (c), 60 (d), 60 (e), 100 (f). Parameters of the simulations are the same as in Fig. 7. Now emission of cAMP saturates near the center of the mound when the concentration of cAMP reaches some threshold, in this case $c_{\mu} = 1900$, so a flat tip is formed at the later stages (d–f) in agreement with experiments.

Our main result concerns the weakening of signaling and chemotactic response of amoeba cells in loose aggregates – this is, within our model, a necessary consequence of the observed mound morphology. Conversely, then, if one finds a mechanism whereby cells lose their adaptiveness to high cAMP, one would predict that the loose aggregate morphology would be measurably different. Of course our results come with a variety of caveats, due to simplifications we have

adopted in this effort. The primary shortcoming of our approach to date is the assumption that there are no significant (in the sense of providing directional information) vertical chemical gradients in the loose mound. Our simulated cells, therefore, are not “dissuaded” in any way from climbing and thereby making the mound grow upward. Next, we have simulated target patterns; mounds that arise from spiral waves might have a tendency to exclude cells from a region the size of the

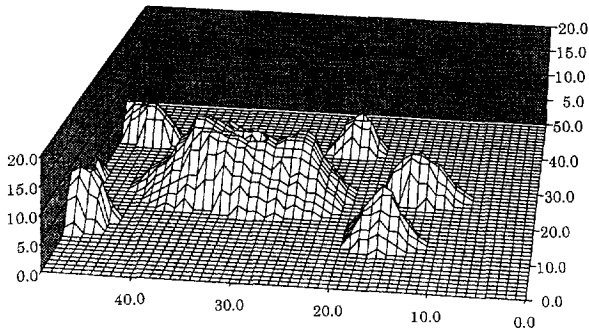


Fig. 8. Final stage of mound formation in the simulation with smaller upper threshold $c_u = 1200$ (all other parameters of simulations are the same as in Figs. 7 and 9). Chemotaxis is suppressed too early along the evolution path, and some cells are not incorporated into the central region of the mound.

core of the spiral merely because of the non-radial orientation of the chemical wavefronts. Since target patterns are typically seen in experiments with low cell density, we do not view this as a serious limitation. Also, our cell mass is incompressible, whereas the actual mound might exhibit density variations; our attempts at incorporating limited compressibility did not alter our findings. Finally, we have completely ignored the details of amoeboid motion as our cells are single points. This is clearly not sensible for cell type sorting where relative motions within a mound alter the distribution of cell type without changing the overall cell density field. We hope that this radical approximation does not destroy qualitative features of the patterns that can be formed with a given set of biological mechanisms, but only additional research will be able to validate or invalidate this concept.

Recently, experimental evidence has shown that cells move about fairly randomly in the early mound stage (talk given at Dicty 95, Dourdan, France, see also [29]⁹). This means that the cells are for some reason unable to follow en masse directional clues arising from any chemical wave. This could be due to a variety of causes – the chemical wave may become too disorganized to affect ordered motion (but this did not happen in our model as shown

above), the cells may not be able to move chemotactically within a multicellular mass of cells, there may be additional chemical signaling or, as we feel is most likely (and hence what we have incorporated into our model), the high levels of cAMP leads to receptor saturation and therefore to a slowing down of chemotactic aggregation. In any event, these results suggest that our simulational results are at least consistent with existing data. Moreover, based on our numerical results, we can suggest certain biological experiments which can discriminate among possible factors responsible for morphology transition.

To test our ideas, one would have to use carefully engineered mutant cell-lines. It is well known that there are variety of cAMP receptors (and a variety of promoters) with different affinities. One possibility would be to express a low affinity receptor (e.g. *car2* [30]) under the usual high affinity (*car1*) promoter, in addition to keeping fixed the *car1* expression. Cells also expressing *car2* might not show the strong cAMP adaptivity and hence might be able to move chemotactically inside the loose aggregate. Of course, if the lack of directed motion is due to locomotion constraints or other chemical signals, we will not get anything new by constructing this cell-line.

Assuming that our modeling approach is providing reliable information, there are several directions available for future research. One can investigate spiraling in mounds with spiral chemical waves – here some experiments show the interesting phenomenon of the re-emergence of orderly cell motion as the mound progresses to later developmental stages. One could study existing mutants such as those which do not express *lagC* [31], which cease development at the early mound stage and in fact reverse some aspects of morphogenesis. Finally, the simulation can be extended to include cell differentiation and one could begin to study sorting with a variety of possible mechanisms to test. This will push modeling into direct contact with the edge of current biological knowledge, a situation with hopefully beneficial consequences for all concerned.

⁹ We have obtained similar results in our preliminary experiments on cell motion within mounds.

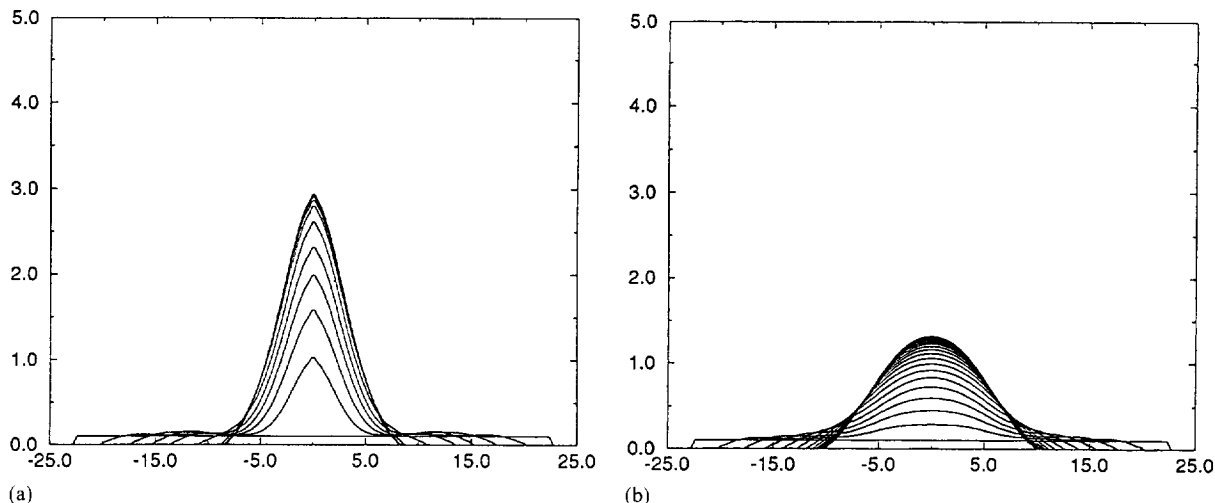


Fig. 9. (a) Simulation of mound formation within our simple mean-field equation (2), with the constant flux $J_0 = 0.1$ (sharp mound); (b) $J_0 = 0.1$ at $r < a$, and $J_0 = 0.1r/a$ at $r > a$ with $a = 5$ (flat mound). Multiple lines correspond to different time steps.

Acknowledgements

We would like to thank W. Loomis and G. Shaalsky for much input regarding Dictyostelium dynamics. We also acknowledge useful discussions with C. Weijer. The cell-line which expresses GFP driven by the actin-15 promoter was obtained from R. Kay.

Appendix A

One can analyze the behavior of our models by appealing to a simple mean-field description of the process of mound growth. Let $h(r)$ be the height of the mound, assumed to be circular. The surface relaxation mechanism that we have used corresponds to moving particles which are on the surface so as to maximize the number of adhesive contacts. In an average sense, the number of such contacts varies as the curvature of the surface

$$\kappa(r) \simeq -\nabla_r^2 h(r),$$

where only the radial components of the Laplacian operator act on the azimuthally symmetric height function h . The flux arising from this would therefore take the form

$$\mathbf{J} = \nabla \kappa.$$

With chemotaxis, there is an additional radial inward particle flux. Assuming that the chemical signal is always sufficient to induce motion, we expect this additional flux to be $\mathbf{J}_c \simeq -J_0(r)\hat{r}$, where J_0 is roughly constant as we approach $r = 0$. The height changes due to the divergence of the flux, leading to the evolution equation

$$\frac{\partial h(r)}{\partial t} = \frac{J_0}{r} - \nabla_r^2 h(r). \quad (\text{A.1})$$

The physical reason for the $1/r$ dependence of the flux term is that the flux is contributing to the height change of an ever narrowing region as $r \rightarrow 0$. In other words, assuming a constant flux magnitude J_0 gives rise to singular behavior in the flux divergence which enters into the height equation. It is rather straightforward to simulate this equation starting from a compact region having J_0 constant $\neq 0$; the results are shown in Fig. 9(a), and agree qualitatively with what our Dictyostelium model always produced without an adaptive mechanism.

Given this simplified understanding, it is clear that flat-topped mounds require that the net flux J_0 go to zero as we approach the mound center. As far as the

simplified model is concerned, we can see this by having J_0 vary as r for $r < a$; the results are shown in Fig. 9(b). This insight was then incorporated into the modified particle simulation, as discussed in the text.

References

- [1] W.F. Loomis, ed., *The Development of Dictyostelium discoideum* (Academic Press, New York, 1982); J.T. Bonner, *The Cellular Slime Molds* (Princeton University Press, Princeton, NJ, 1967); P. Devreotes, *Science* 245 (1989) 1054; P.C. Newell, in: *Biology of the Chemotactic Response*, ed. J.M. Lackie (Cambridge University Press, Cambridge, 1981); M. Darman and P. Brachet in: *Taxis and Behavior*, ed. G.L. Hazelbauer (Chapman and Hall, London, 1978).
- [2] D.K. Tomchik and P. Devreotes, *Science* 212 (1981) 443; F. Alacantha and M. Monk, *J. Gen. Microbiol* 85 (1974) 321.
- [3] H. Levine and W. Reynolds, *Phys. Rev. Lett.* 66 (1991) 2400.
- [4] B.N. Vasiev, P. Hogeweg and A.V. Panfilov, *Phys. Rev. Lett.* 73 (1994) 3173.
- [5] T. Hofer J.A. Sherratt and P.K. Maini, *Proc. Roy. Soc. B* 259 (1995) 249.
- [6] M. Steinberg, *J. Theor. Biol.* 55 (1975) 431.
- [7] W. Ward, *Photochemical and Photobiological Reviews*, ed. K. Smith, Vol. 4 (Plenum Press, New York, 1979); M. Chalfie, Y. Tu, G. Euskirchen, W. Ward and D. Prasher, *Science* 263 (1994) 802.
- [8] K.W. Doolittle, I. Reddy and J.G. McNally, *Dev. Biol.* 167 (1995) 118.
- [9] D. Kessler and H. Levine, *Phys. Rev. E* 48 (1993) 4801.
- [10] H. Levine, *Chaos* 4 (1994) 563.
- [11] H. Parnas and L. Segel, *J. Cell. Science* 25 (1977) 191. *J. Theor. Biol.* 71 (1978) 185; S.A. Mackay, *J. Cell. Science* 33 (1978) 1.
- [12] O. Vasieva, B. Vasieva, V. Karpov, A.N. Zaikin, *J. Theor. Biol.* 171 (1994) 361.
- [13] E.F. Keller and L.A. Segel, *J. Theor. Biol.* 26 (1970) 399; V. Nanjundiah, *J. Theor. Biol.* 42 (1973) 63.
- [14] R. Kay, *Curr. Opin. Gen. Dev. Biol.* 4 (1993) 637; W.F. Loomis, *Curr. Topics in Dev. Biol.* 28 (1994) 1.
- [15] M. Sussman, *Meth. Cell. Biol.* 28 (1987) 9.
- [16] R. Clark and T. Steck, *Science* 204 (1979) 1163.
- [17] F. Siegert, C. Weijer, A. Nomura and H. Miike, *J. Cell. Science* 107 (1994) 97.
- [18] O. Steinbock and S. Muller, *Zeit. Fur Natur. C* 50 (1995) 275.
- [19] W. Loomis, unpublished results.
- [20] H. Levine, I. Aranson, L. Tsimring and T.V. Truong, *Proc. Nat. Acad. Science* 93 (1996) 6382; see also I. Aranson, H. Levine, and L. Tsimring, *Phys. Rev. Lett.* 76 (1996) 1170.
- [21] R. Goldstein, K. Lee and E. Cox, *Phys. Rev. Lett.* 93 (1996) 6382.
- [22] P.N. Devreotes and S.H. Zigmond, *Ann. Rev. Cell. Biol.* 4 (1988) 649.
- [23] D.A. Kessler, H. Levine and L.M. Sander, *Phys. Rev. Lett.* 69 (1992) 100.
- [24] J.-L. Martiel and A. Goldbeter, *Biophys. J.* 52 (1987) 807.
- [25] Y. Tang and H.B. Othmer, *Math. Biosci.* 120 (1994) 25.
- [26] L. Wu and J. Franke, *Gene* 91 (1990) 51.
- [27] E. Ben-Jacob et al., *Nature* 368 (1994) 46.
- [28] W. Loomis, private communication.
- [29] C. Weijer, private communication.
- [30] C. Saxe, G. Ginsburg, J.Y. Louis, R. Johnson, P. Devreotes and A.R. Kimmel, *Genes and Develop.* 7 (1993) 262.
- [31] J. Dynes et al., *Genes and Develop.* 8 (1994) 948.